NASA
Technical
Paper
2016

June 1982

Approximate Analysis of Thermal Convection in a Crystal-Growth Cell for Spacelab 3

Robert F. Dressler

NASA

NASA Technical Paper 2016

1982

Approximate Analysis of Thermal Convection in a Crystal-Growth Cell for Spacelab 3

Robert F. Dressler
NASA Office of Space Science and Applications
Washington, D.C.

NASA
National Aeronautics and Space Administration

Scientific and Technical Information Branch

Introduction

The first Materials Processing in Space (MPS) experiment scheduled by NASA for a Spacelab flight will investigate the production of more homogeneous crystals, free from inclusion of solution, by suppression of thermal convection because of the almost 0-g environment. This experiment, being monitored at NASA-Marshall Space Flight Center has Drs. R. B. Lal, R. L. Kroes, and W. Wilcox as principal investigators, and will be flown in the Fluids Experiment System (FES), scheduled for Spacelab 3.

A crystal of triglycine sulfate (TGS) will be grown at the center of a cubical box containing liquid. This cube is 10 cm on a side, and its walls are held at a fixed temperature T_H. The growing TGS crystal, which we specify here to have 1 cm^3 volume (its approximate shape whether taken as a cube or sphere, etc. not being of much significance for this analysis) is held at the center of the cubical container by a support attached to the center of one face (Fig. 1). The support carries a cooling system which maintains the crystal at a fixed temperature T_c which is 10°C less than the fixed wall temperature T_H. This temperature difference ΔT in the presence of small (but not zero) variable acceleration fields during orbital flight will set up slow thermal convective currents in the liquid. Since the magnitude and location of these currents can adversely affect the quality of the growing crystal, it is important to have some advance quantitative estimate of these.

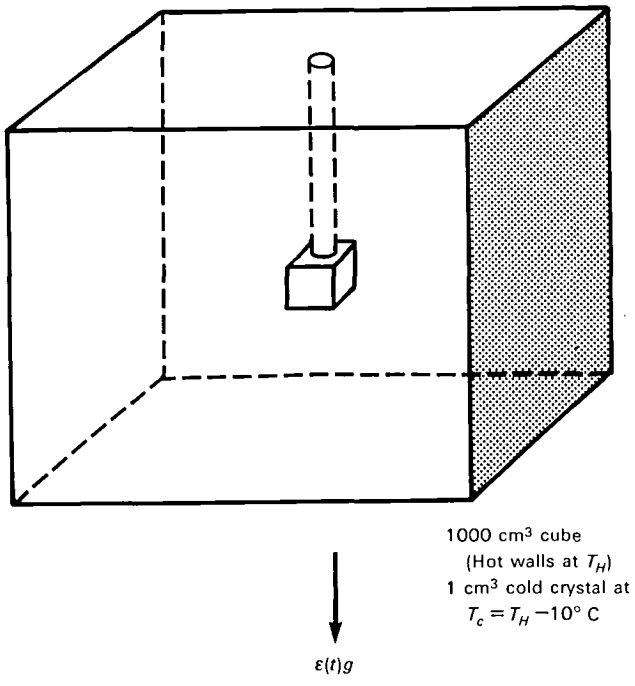

Figure 1.—Three-dimensional convection in Spacelab MPS experiment.

Approximate Analytical Method

Before a complete computational analysis finally will become available for this problem, we have made the following rough preliminary theoretical analysis in terms of known analytical solutions for convection in much simpler models. Analytical solutions were already available for 2-dimensional (2-D) steady convection in a square (Batchelor [1]) and in a circle (Weinbaum [2]), and for the transient solution for a circle (Dressler [3]) in which it was indicated that the transient and steady solutions for the circle were also applicable to the major central region of a square of equal area. Although the TGS configuration is a much more complicated geometry and produces 3-D flow, a rough estimate can nevertheless be made which will be described here. If any such estimates get within even one order-of-magnitude of the true velocities, it is helpful for advanced planning of the experiment.

We consider the cell in Fig. 1 to be subjected to a small acceleration $\varepsilon(t)g$ directed downwards where $\varepsilon(t)$ may define any time-variation. It was shown in [3] that a transient convective response to any $\varepsilon(t)g$ can be obtained by appropriate combination of the basic transient due to a step-function acceleration. We will show furthermore that we will require an estimate only for the basic step-function transient for the TGS cell. One notes in Fig. 1 that the convection will be slightly different depending upon the orientation of the εg vector, due both to the cubical geometry of the cell, and also to the small barrier created by the support rod for the crystal. Our first simplification will be to ignore this support. Secondly, since it is known that at low Rayleigh numbers convection in a square, except close to the corners, is almost identical with convection in a circle of equal area ([1], [2], and [3]), by analogy we will therefore replace the cubical cell by a spherical cell of equal volume. If we now consider the small crystal to be a sphere of 1 cm^3 volume, we see (Fig. 2) that the flow pattern will be identical for any fixed orientation of the εg vector. We therefore can take it downward in Fig. 2 without loss of generality. The flow pattern for

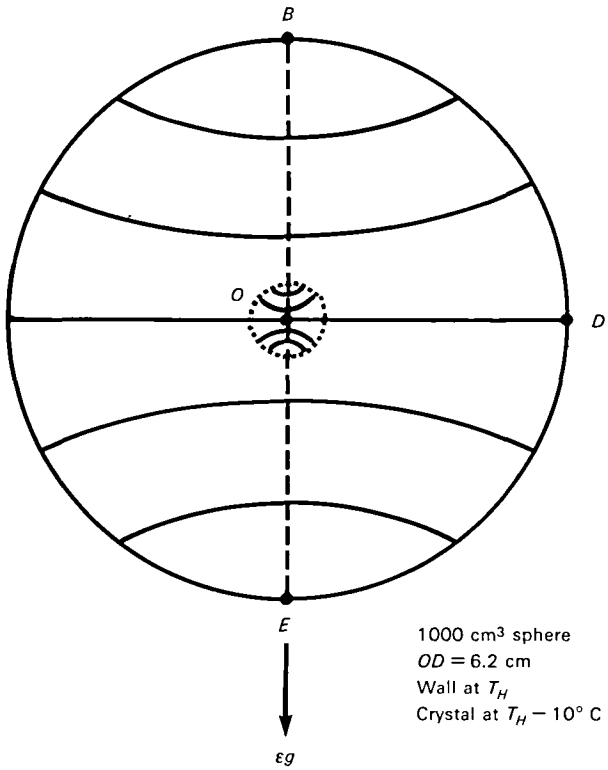

Figure 2.—Spherical container of equal volume.

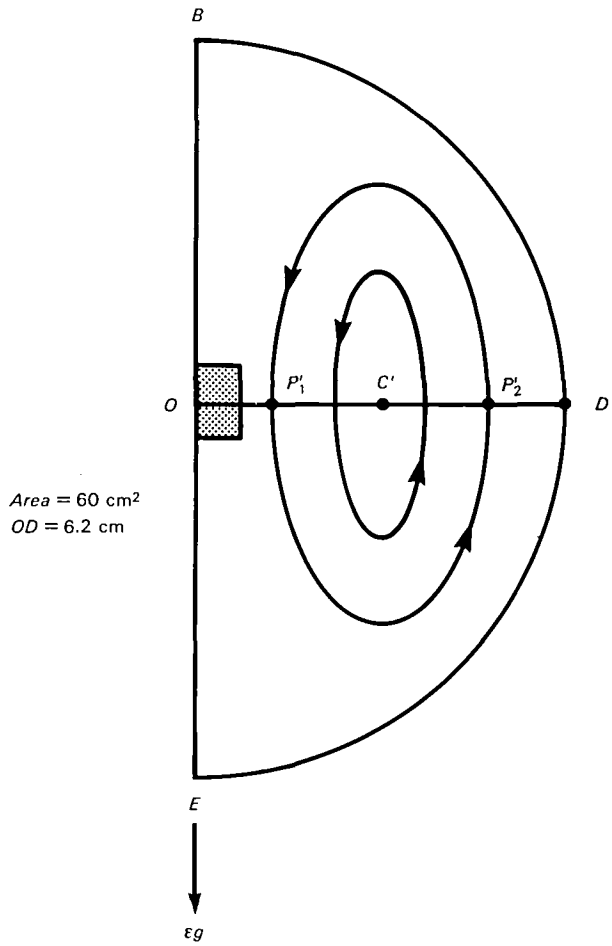

Figure 3.—Streamlines of rotationally symmetric flow in any planar section of the sphere.

this fixed εg will be rotationally symmetric with respect to the vertical diameter *BOE*, and can then be studied in the semicircular plane area *BOED* (Fig. 3).

In [3] there was automatic linearization of the basic equations due to the 2-D circular symmetry. In the Fig. 2 case, however, the basic 3-D equations are not linear for the symmetric flow, but we can linearize them because of the very low velocity in this problem. Thus, only the step-function solution for Fig. 2 will be needed to solve for any transient, by forming appropriate linear combinations with phase lags, as demonstrated in [3].

Although all quantities could easily be put into dimensionless form, we will retain dimensions in order to describe the specific cell, crystal size, and temperature difference in this experiment. The magnitude of εg could be taken arbitrarily for the step-function acceleration, subject only to the condition that the Rayleigh number remains small in order to guarantee validity of our analytical solutions to be used (see [3] where an upper limit of 6500 was imposed for steady state). We will specify $\varepsilon g = 10^{-6} g$ which corresponds, for example, to the effect of a strong aerodynamic drag on the Shuttle in orbit. The flow velocities for any other value can be obtained immediately since they are directly proportional to the acceleration in this range. For MPS experiments the Rayleigh numbers are usually very low. In such cases convection patterns take the simplest shape, in our case a single circulation pattern as shown in Fig. 3. This flow must be counterclockwise since the left boundary *BOE* is cooler than the boundary *BDE*. For equal spherical and cubical volumes $OD = 6.2$ cm and the area for the semicircular domain is $A = 60$ cm^2. Although the flow may be visualized in the typical plane *BOED*, it is of course rotationally symmetric, not two-dimensional. Our procedure in this approximate analysis, however, will be to consider first a 2-D flow in *BOED*, then later this flow will be geometrically modified to account approximately for the 3-D rotational symmetry in the sphere.

We return now to considering the crystal as a cube of 1 cm^3 volume, and therefore consider a slab slightly thicker than 1 cm (in order to enclose fully the half-cube representing half the crystal) with the semi-circular cross-section *BOED*, inside which we now consider a strictly 2-D flow (Fig. 4). The half-cube crystal is held at temperature T_c while the semicircular lateral surface is at T_H where $T_H - T_c = 10°C$. The flat surfaces on the left boundary above and below the crystal are not

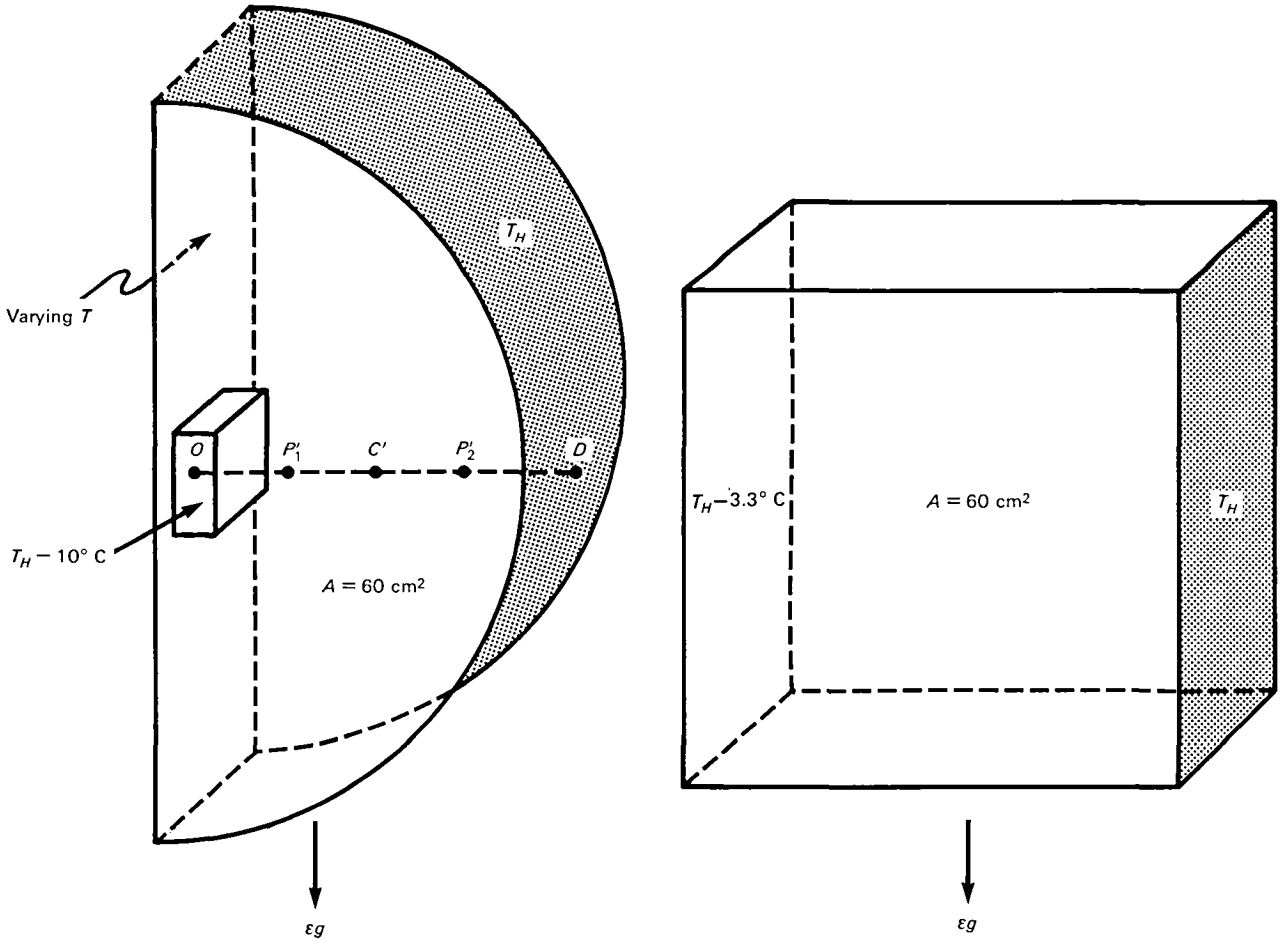

Figure 4.—Replacement of semicircular domain by a square.

material boundaries, but consist of liquid which by symmetry cannot flow through these areas, but only parallel to them. In convection problems for very low Rayleigh numbers, it was shown in [3] that it is sufficient to approximate the thermal field in the moving liquid by the undisturbed thermal field if there were no convection. The undisturbed thermal field in our spherical model (Fig. 2) consists of concentric spheres for the isothermal surfaces, and with the temperature varying inversely with radial distance from the center. The constant temperature distribution on these left boundaries is therefore known and given approximately by

$$\Delta T = 0.88 - 5.44/r \quad °C \tag{1}$$

while the lateral surfaces of the crystal are at

$$\Delta T = -10°C. \tag{2}$$

Since the total heat flux through the cell is the excitation driving the thermal convection, we can next replace the variable temperature distribution on the entire left bounding surface (including all five faces of the crystal half-cube) by its average value and still retain the same total heat flux. A calculation using both (1) and (2) gives

$$\Delta T_{av} = -3.3°C \text{ (on total left boundary).} \tag{3}$$

In addition to the previously noted interchangeability of a square and circle, not only for steady convection but also for the transients (Robertson & Spradley [4]), it has been observed much more generally (Spradley [5]) that for equal areas and the same ΔT imposed across the width, any specific geometric shape of the enclosure is, within reasonable bounds, only of slight importance upon the 2-D convection in the central region. We therefore replace the semicircular slab (which now has a constant temperature difference ΔT_{av} imposed upon its entire left boundary surface) by a square slab with equal face area (60 cm²) as shown in Fig. 4. In both slabs, the front and rear faces are not material boundaries and exert no drag upon the 2-D

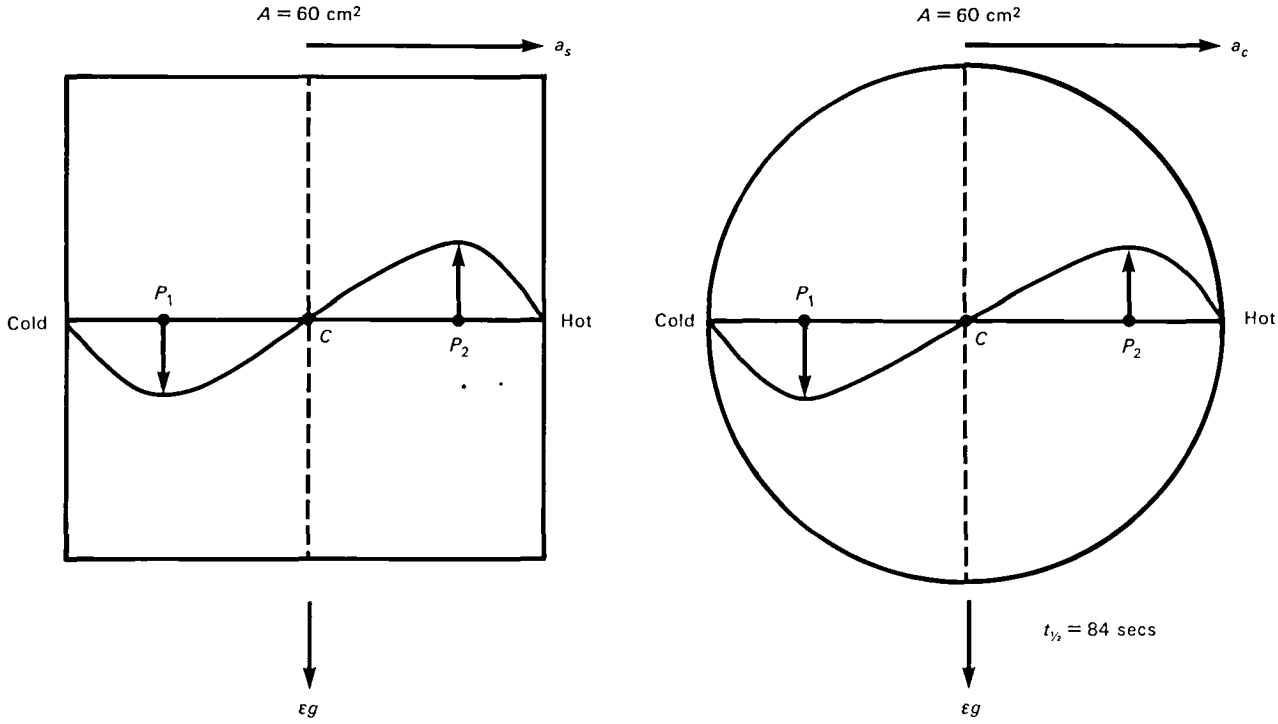

Figure 5.—Two-dimensional thermal convection in square and equivalent circle.

flows. For a more precise replacement the upper and lower edges of the square slab should be held at T_H also, but it is known from many calculations ([4] and [5]) that the thermal boundary conditions on upper and lower edges play only a minor role in the central convection, compared with the temperatures imposed upon the vertical edges. Thus, if we allow the imposed temperatures on the horizontal sides to be linearly varying between the two vertical sides, we have now produced a square model with a known solution [1] for the steady convection, and with an accurate approximate solution also known for the transient convection [4]. In the above argument, it would be more precise for a 2-D flow in the Figure 4 model to have taken a narrower slab which excludes the front and back faces of the crystal. These were incuded, however, in the calculation for the result (3) to compensate for the neglect of the "slip" boundary condition on the left boundary above and below the crystal. A more lengthy analysis which excludes the two crystal faces but introduces the "slip" condition yields essentially the same final result for convective velocities along *OD*, and is therefore omitted for brevity.

Along either major axis of a square and along any radius of a circle, if r/a is the dimensionless distance from the center, the steady convective velocity varies as the quantity $r/a - (r/a)^3$ as shown in Fig. 5, and with the velocities at corresponding points equal in magnitude when the face areas are equal. Maximum velocity is at the locations $r/a = \pm 0.58$ and these locations are designated by P_1 and P_2.

The 2-D transient solution for a step-function εg applied at $t = 0$ for the circle [3] is

$$v^B(r, t) = \frac{\varepsilon g \cos\phi}{16} \frac{\Delta\rho}{\rho} \frac{a^2}{\nu} \left[\frac{r}{a} - \left(\frac{r}{a}\right)^3 + 16 \sum_1^\infty \frac{J_1(\lambda_n r/a)}{\lambda_n^3 J_0(\lambda_n)} \exp\left(-\lambda_n^2 \frac{\nu}{a^2} t\right) \right]. \quad (4)$$

which is likewise almost identical [4] with the 2-D transient velocity along a major axis of a square of equal area. Here $2\Delta\rho$ is the density difference over the width of the enclosure, and λ_n is the n-th root of the Bessel function $J_1(x)$. The half-time build-up is given approximately by the exponential in the first term with e^{-1}, and is

$$t_{½} = 0.068 a^2/\nu. \quad (5)$$

For our TGS liquid, viscosity $\nu = 1.5 \times 10^{-2}$ cm²/sec, the thermal expansion coefficient $\beta = 2.07 \times 10^{-4}$/°C, thermal diffusivity $\kappa = 1.24 \times 10^{-3}$ cm²/sec, and the (equal-area) circle radius is $a = 4.37$ cm, giving

$$t_{½} = 84 \text{ secs}. \quad (6)$$

At steady 2-D flow (4) gives

$$v^{SS}(P_1 \text{ and } P_2) = 0.1 \text{ micron/sec.} \qquad (7)$$

We now identify the known 2-D flow in the central region of the square model in Figs. 4 and 5 with the 2-D flow in the central region of the semicircular slab of equal face area shown on the left side of Fig. 4. We temporarily disregard the projecting crystal, and identify the points P_1', C', *and* P_2' on the line *OD* in Figs. 3 and 4 to correspond to P_1, C, and P_2 in Fig. 5, with C' at the center of *OD*, and with P_1' and P_2' at 0.58 of the distance from C' to O and to D, respectively.

These velocities refer of course to purely 2-D flow. The final step is to adjust approximately these 2-D results by a geometrical consideration to apply to the rotationally symmetric flow in the model of Fig. 2. If we pass a horizontal plane containing *OD* through the sphere of Fig. 2, and look down at a wedge-shaped section on this plane (Fig. 6), we note that the width of the cross-section of any streamtube must, because of the rotational symmetry, vary linearly with its distance from the point of the wedge. Since the width of any streamtube cross-section is constant in the 2-D flow inside our slab of constant width (dashed lines in Fig. 6), we consider the geometrical effect due to mass conservation on the established and known 2-D flow if we now distort this flow by rotating the two walls *FG* and *HK* about the points *M* and *N*, respectively, in order to create the wedge domain *QOR*. The resulting section of a rotationally symmetric flow must have increased velocity in the regions where the streamtube width is narrowed, and decreased velocity where it is broadened. The velocities of the incompressible fluid must therefore be adjusted inversely to the new width of the streamtube. For example, at P_1' the 2-D velocity must be multiplied by the factor 2.5, and by the factor 0.63 at P_2'. Approximate 3-D results therefore for the rotationally symmetric flow for Figs. 2 and 3 are, using (7) for the steady flow,

$$v^{SS}_{max} = v^{SS}(P_1') = 0.25 \text{ micron/sec.} \qquad (8)$$

$$v^{SS}(P_2') = 0.064 \text{ micron/sec.} \qquad (9)$$

To obtain the transient flow as a function of t, for the step function at any point such as P_1', we multiply the transient curve for the circle [3] evaluated at the corresponding point by the appropriate geometrical factor at every time value. For example, the result at P_1' is shown in Fig. 7, as the dashed curve.

Our reasoning above is somewhat related to that used in the theory of Kinematic Waves (Lighthill & Whitman [7], Whitman [8]). In that theory the solution is obtained by solving only the mass conservation equation, without coupling the dynamical equation with it. Instead, a known relation must be employed (the "density vs. flux" relation) which replaces the solution to the exact dynamical equation. In our approach, the wedge flow is obtained from the mass equation by using a previously obtained result from other approximate dynamical considerations.

It is obvious that our above geometrical approach will not remain valid when the weighting factor departs widely from unity, i.e., in the region of the sharp point of the wedge, where the factor goes towards infinity. There the resulting gradients and stresses would become so large that the correct dynamical equations could not be ignored. Also, this region is not relevant to our basic problem since it includes the crystal which we temporarily ignored. The domain for using the approximation can be terminated as follows: We expect that the two

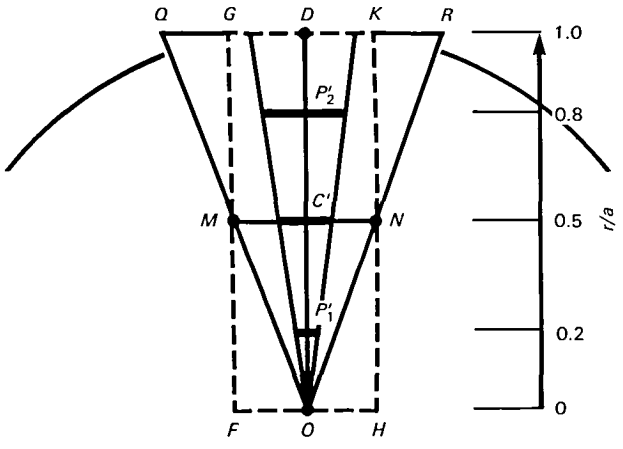

Figure 6.—Geometrical adjustment of the flow by mass conservation.

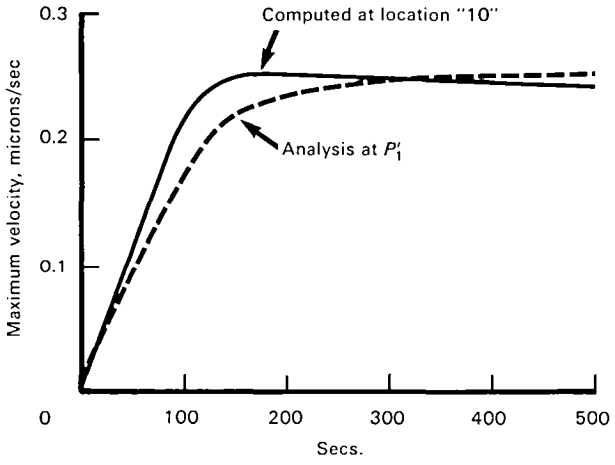

Figure 7.—Step-function transient.

positions for maximal velocity in the wedge flow will not be significantly displaced from the locations P_1' and P_2' determined from the 2-D flow. We will therefore retain results from the mass-conservation argument up to the point P_1' where we will take the velocity to be a maximum. From there, a simple linear interpolation can be made to the crystal surface location X where the velocity is known to be zero.

Discussion of Results

Our analysis was finished months before any computer results were available, but computational analysis was later requested and completed (Spradley et al. [6]) on the rotationally symmetric flow of Fig. 2, by considering the flow in Fig. 3 in terms of 2 space variables plus time in spherical coordinates. In the numerical computation, a cylindrical crystal of same volume was included, but not its support rod. For comparison the solid curve in Fig. 7 is the computer result for the step-function transient evaluated at location "10" on Fig. 9 (the maximum velocity location), and the computed half-time is 70 secs. Our estimate in (6) was 84 secs.

The Rayleigh number N_R for the models in Fig. 5 is defined as

$$N_R = \varepsilon g \frac{2\Delta\rho D^3}{\rho\nu\kappa} \tag{10}$$

which for our problem has the low value about

$$N_R = 24. \tag{11}$$

We will also associate this value with our original problem shown in Fig. 1, since for that type of container-and-crystal geometry, a Rayleigh number definition is not standardized. This very low value of 24 guarantees that each analytical solution used in this analysis is very accurate.

Fig. 8 reproduces the computational results in [6] for the direction of the velocity vectors in the steady rotationally-symmetric flow in Fig. 3, but the direction of the acceleration vector is here taken horizontally to the left. After a 90° rotation, this figure becomes the mirror image of Fig. 3. We note the computed sense of circulation agrees with our assumption, viz. in the direction of εg near the crystal, and oppositely near the outer boundary. The computed position of C of the center of circulation where the velocity vanishes is seen to be very close to our predicted location C'. Fig. 9 reproduces from [6] the corresponding computational results for the velocity magnitudes in the steady flow. This shows the maximum velocity at location "10" to be 0.23 micron/sec, and is very close to our predicted point P_1'; and it shows 0.08 micron/sec at the position of our point P_2'. The slight displacement of location "10" from the axis OD is probably numerical error rather than an indication of any flow asymmetry.

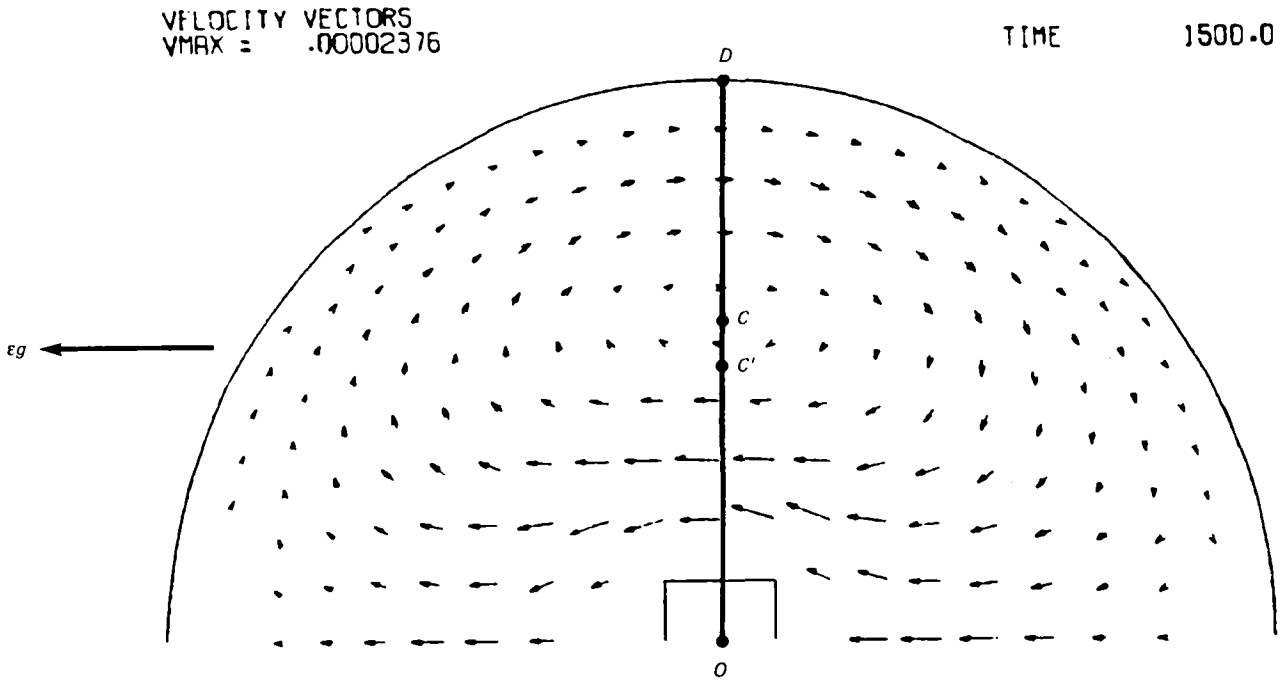

Figure 8.—Lockheed simulation of Lal experiment—velocity vectors at steady flow.

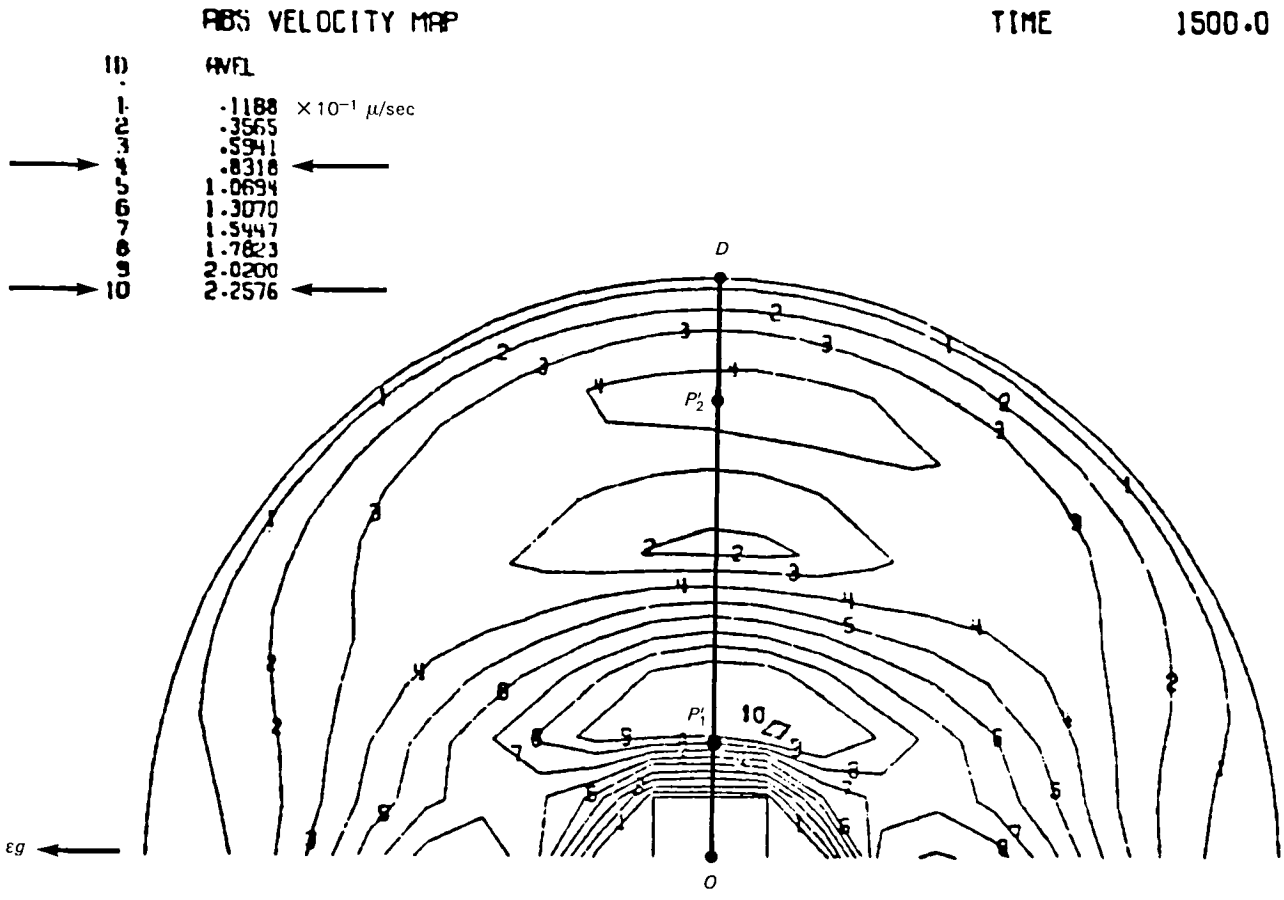

Figure 9.—Lockheed simulation of Lal experiment—velocity map. Velocity magnitudes at steady flow.

Fig. 10 shows our results (dashed line) for the steady-state velocity distribution along line *OXD* compared with the numerical results (solid line). This comparison is based in both approaches upon the rotationally symmetric convection defined by the model in Fig. 2.

These dimensional final results for the specific cell analyzed here can immediately be transformed, if desired, into dimensionless form for application to other sizes of cell-and-crystal of similar geometry, with different ΔT, εg, and liquids, by using the same parameter groups given in (4) and (5), and subject to the known restriction on size of the Rayleigh number as defined in (10).

The replacement of the cubical model (Fig. 1) by the equal-volume spherical model (Fig. 2) is the only step in our analysis which cannot be supported by an argument based upon some known results or procedures; it is an assumption for 3-D flow at low Rayleigh number made by analogy with the known equal-area results for 2-D flow. Numerical results are not yet available for the slightly non-symmetric flow created by the

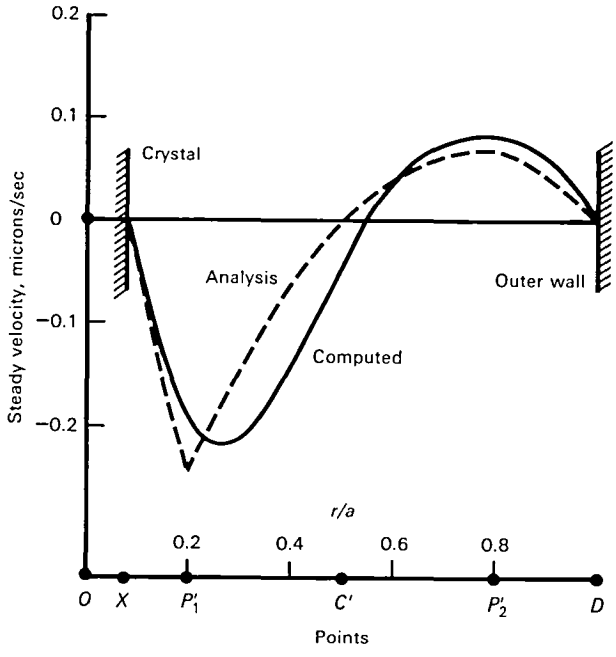

Figure 10.—Velocity distribution along radius *OD*.

model in Fig. 1 with the cubical container and the crystal support. This will be a much more difficult and costly computation which must use 3 independent space variables plus time. It is anticipated, however, that a complete 3-D computational analysis will yield flow patterns and maximum velocities which will differ very little from the approximate results we have already obtained.

Conclusions

Our quantitative results can be interpreted better by making a comparison with the convection in a more commonly used model (with the same specified parameters) as follows: If we imposed the $\Delta T = 10°C$ between the left and right faces of the cube in Fig. 1 (without crystal or support) and neglect the small, local effect of drag from the front and back faces, the resulting 2-D steady convection would have [3] peak velocity $v_{max}^{SS} = 0.5$ micron/sec, and $t_{½} = 140$ secs. By comparison, results presented here for the Fig. 2 model are 0.22 to 0.25 micron/sec and 70 to 84 secs., respectively, which constitute more than 50% reduction in velocity, but with a response time twice as rapid, compared with the standardized model.

The model in Fig. 1 or 2 differs in three basic respects from our standard: (1) its lateral surface (the crystal) where the ΔT is imposed has much smaller area which lowers the convective velocities, (2) its linear dimension *OD* within which the circulation cell is confined is much smaller, which reduces the velocity, but speeds up the response time, (3) the rotational symmetry in the flow, because of the wedge effect, increases velocities near the crystal where the peak velocity occurs. The overall result of these three effects combined is to reduce peak velocity but to speed up the response time, compared with the reference model.

The results for the steady-state velocities and the response time $t_{½}$ to a step-function εg will now permit construction of the transient solutions at any point along *OD* caused by any arbitrary, time-varying acceleration, following the procedure presented in [3].

The rough and partly heuristic analysis described here was undertaken to obtain preliminary quantitative estimates of the thermal convection to be expected in this specific MPS experiment. Since computer results subsequently became available for the Figure 2 model which confirmed the accuracy of our approximate analysis, this description of our approach has been made available so that other complicated MPS geometries can be analyzed easily and quickly for preliminary predictions useful in engineering planning. In particular, an application to thermal convection in microgravity for cylindrical float-zones is in progress.

References

[1] G. K. Batchelor, Quart. Appl. Math., Vol XII, No. 3 (1954)

[2] S. Weinbaum, J. Fluid Mech., Vol 18 (1964)

[3] R. F. Dressler, J. Crystal Growth, 54 (Sept. 1981)

[4] S. J. Robertson & L. W. Spradley, Tech. Report D-697821, Lockheed Missiles and Space Co., Huntsville, AL (Aug. 1980)

[5] L. W. Spradley, private communication. To appear in Lockheed Tech. Report D-784759.

[6] L. W. Spradley, L. A. Nicholson, & S. J. Robertson, Tech. Report D-784480, Lockheed Missiles and Space Co., Huntsville, AL (Aug. 1981)

[7] M. J. Lighthill & G. B. Whitham, Proc. Royal Soc., A 229 (1955)

[8] G. B. Whitham, Linear & Non-Linear Waves, John Wiley & Sons, New York (1974)

1. Report No.	2. Government Accession No.	3. Recipient's Catalog No.
NASA TP-2016		

4. Title and Subtitle	5. Report Date
APPROXIMATE ANALYSIS OF THERMAL CONVECTION IN A CRYSTAL-GROWTH CELL FOR SPACELAB 3	June 1982
	6. Performing Organization Code: EN–1
7. Author(s): Robert F. Dressler	8. Performing Organization Report No.
	10. Work Unit No.
9. Performing Organization Name and Address: Materials Processing in Space Office, NASA, Office of Space Science and Applications, Washington, D.C. 20546	11. Contract or Grant No.
	13. Type of Report and Period Covered: Technical Paper
12. Sponsoring Agency Name and Address: National Aeronautics and Space Administration, Washington, D.C. 20546	14. Sponsoring Agency Code

15. Supplementary Notes

16. Abstract

A general approach, flexible in scope, is described here for estimating analytically the transient and steady thermal convection in microgravity. The approach is applicable to many 3-dimensional flows in containers of various shapes with various thermal gradients imposed. The method employs known analytical solutions to 2-dimensional thermal flows in simpler geometries, and does not require recourse to numerical calculations by computer. The approach is illustrated by describing a specific application to a contemplated NASA experiment in space.

17. Key Words (Suggested by Author(s))	18. Distribution Statement
Thermal convection Crystal growth Low-*g* processing	Unclassified—unlimited Subject category 12

19. Security Classif. (of this report)	20. Security Classif. (of this page)	21. No. of Pages	22. Price
Unclassified	Unclassified	9	A02

For sale by the National Technical Information Service, Springfield, Virginia 22161

NASA-Langley, 1982

National Aeronautics and Space Administration

Washington, D.C.
20546

Official Business
Penalty for Private Use, $300

SPECIAL FOURTH CLASS MAIL
BOOK

Postage and Fees Paid
National Aeronautics and
Space Administration
NASA-451

NASA

POSTMASTER: If Undeliverable (Section 158 Postal Manual) Do Not Return